Molecular Crystals and Liquid Crystals
Publication details, including instructions for authors and subscription information:
http://www.tandfonline.com/loi/gmcl16

NMR and Raman Scattering Studies of MBBA and EBBA

Munehisa Yasuniwa [a b], Seiji Taki [a] & Tetuo Takemura [a]

[a] Department of Applied Science, Faculty of Engineering, Kyushu University, Fukuoka, 812, Japan

[b] Kurume National Technical College, Komorinomachi, Kurume Fukouka, 830, Japan

Version of record first published: 20 Apr 2011.

To cite this article: Munehisa Yasuniwa , Seiji Taki & Tetuo Takemura (1980): NMR and Raman Scattering Studies of MBBA and EBBA, Molecular Crystals and Liquid Crystals, 60:1-2, 111-132

To link to this article: http://dx.doi.org/10.1080/00268948008072428

Mol. Cryst. Liq. Cryst., 1980, Vol. 60, pp. 111–132
0026-8941/80/6001-0111$04.50/0

Printed in the U.S.A.

NMR and Raman Scattering Studies of MBBA and EBBA

MUNEHISA YASUNIWA,† SEIJI TAKI and TETUO TAKEMURA

Department of Applied Science, Faculty of Engineering, Kyushu University, Fukuoka 812, Japan

(*Received July 9, 1979; in final form November 11, 1979*)

The refined broad line NMR spectra of MBBA and EBBA and the Raman spectra in the low frequency region (100 ~ 650 cm^{-1}) of EBBA are given. The band associated with the accordion mode vibration of the end butyl chain of these molecules is assigned to 280 cm^{-1} in Raman spectrum. The analysis of accordion mode vibration indicate that the end butyl chain EBBA molecule tends to take all trans conformation, and that that of MBBA molecule tends to take the conformation which has constraint, such as gauche conformation. Assuming that the whole molecular conformation of each sample in the nematic phase, assignments between protons attached to each molecule and each line in the NMR spectrum are given. Molecular and segmental motions, molecular packing, and orientational order in the nematic phase of these samples are discussed.

1 INTRODUCTION

N(*p*-methoxy-benzylidene) *p*-n-butylaniline (MBBA) and N(*p*-ethoxy-benzylidene) *p*-n-butylaniline (EBBA) are also Shiff base nematic liquid crystals and have been extensively studied. The chemical structures of these molecules are similar to each other and difference is found only in the alkoxy group. In spite of the similarity of those chemical structures, those physical properties are fairly different from each other. It is seen, for example, in respect of melting and clearing points, specific volume,[1–4] etc. It is supposed that the differences of the molecular conformation play an important role on the physical properties. Many investigators have been employing a broad line NMR method as a useful tool to study a molecular motion in a nematic phase and are obtained a degree of long range molecular

† Kurume National Technical College, Komorinomachi, Kurume, Fukouka 830, Japan.

ordering. On the other hand, laser Raman spectroscopy has been used to elucidate molecular structure and to study intermolecular interaction and molecular conformation at various phases. Some authors[5–12] have already applied this technique as a useful tool to the study of a molecular conformation of nematic liquid crystals. For the investigation of the molecular and segmental motion and conformation in the nematic phase, both broad line NMR and Raman spectroscopy are also useful experimental techniques.

The first to report NMR study on a nematic liquid crystals were Spence and his co-workers,[13,14] who observed a NMR spectrum of PAA. Since then, many NMR spectra of nematic liquid crystals have been presented, but those are generally broad ones. Rather fine resonance spectra has been reported by Loesche,[23] but the S/N ratio of his NMR spectra is not so adequate as he pointed out in his paper and the resonance spectra are not symmetrized. Saupe and Englert[24] have given a detailed NMR spectrum of PAA using high resolution NMR technique. For obtaining the more detailed analysis of the specific dipole–dipole interactions of specific protons, some authors have carried out NMR studies using the method of selective deuteration[14,15,21,22] and fluorination[16] and selective substitution.[18–20,23] There has been no report on refined spectrum of (non-deuterated) MBBA and EBBA and any detailed analysis has not been presented with broad line NMR method. In the first place, more detailed NMR spectra of MBBA and EBBA are needed to explain the segmental and molecular motion in the nematic phase of these materials.

Raman study of nematic material was initiated by Freyman and Servant[5] on PAA, and since then many authors have done their investigations by the use of Raman spectroscopy. However, nematogenic molecule are always complex organic systems, so that those lead to a fairly complicated Raman spectrum, which is not easily interpreted.

In n-paraffin, an accordion mode vibration has been observed.[25,26] The accordion mode vibration of the end chain of nematogenic molecule has been reported by Schnur,[6,7] Vergoten and Fleury[8] and Destrade *et al.*[9,10] Since MBBA and EBBA molecules are partly composed of alkyl benzene segment, Raman measurements is a useful step toward detection of conformational structure of the alkyl chain tail. Schnur has obtained the correlation between the carbon number of alkoxy chain and the vibrational frequency of accordion mode vibration of homologous alkoxy azoxybenzene series. And he has assigned the accordion mode vibration of end butoxy chain to 340 cm^{-1} band. Vergoten *et al.* have already reported the Raman spectra of MBBA in the 100–3200 cm^{-1} region and given the assignment to each band. Normal coordinate analysis of benzylidene aniline has been used for the assignment of skeletal modes of MBBA. And they have asssigned the accordion mode vibration of the end butyl chain of MBBA molecule

to 340 cm^{-1} band. Destrade *et al.*[9] have presented the Raman spectra of MBBA with adequate S/N ratio, and they[10] have assigned the vibrational frequency of all trans conformation of butyl chain to 797 cm^{-1}. Their assignment is based on the variation of its band frequency. On the other hand, accordion mode vibration of the end butyl chain of EBBA molecule has not been reported so far to the best of our knowledge. So in the first place refined Raman spectra of EBBA are needed.

In the present investigation, refined NMR spectra and Raman spectra of MBBA and EBBA are obtained. And the assignment of accordion mode vibration of the end butyl chain is attempted. Segmental and molecular motions of these materials and the conformation of the end butyl chain are analyzed on the basis of these spectra and volumetric and x-ray data.

2 EXPERIMENTAL

2.1 Samples

Highly purified MBBA and EBBA samples were obtained from Fuji Sikiso Co. and therefore these samples were not purified furthermore. EBBA sample, which was used in NMR experiment, was obtained from Tokyokasei Co. and recrystallized three times.

As to solid modifications of MBBA, many authors have already reported by the use of thermal analysis,[29,31] Raman spectroscopy[9,12] and other methods. However, the characterization, classification and transforming process are not consistent to each other. And the crystal lattice, molecular packing and molecular conformation of each solid modification have not been presented. So in the present investigation the heat treatment of the used sample follows the method of Meyer,[29] who has suggested that metastable form at $-3°C$ and above converts spontaneously to the stable form with the libration of heat. The MBBA sample was cooled down from nematic and heated again to 6°C and above, and the sample was annealed for one week held at the same temperature. This sample was used as a solid form of MBBA.

As to solid modification of EBBA, Cavatorta *et al.*[11] have reported three solid modifications with the Raman spectroscopy in the region below 250 cm^{-1}. By the use of thermal analysis Sorai *et al.*[31] and Ogorodnik[32] have also reported the solid modifications. There can be found no coincidence among their results. In this investigation, the author follows the reference (33) in the heat treatment for obtaining stable and metastable solids of EBBA. The EBBA sample was cooled down from nematic to $-10°C$ and heated again up to 32°C and cooled down to the room temperature, and used as a stable solid form.

2.2 Broad line NMR

Samples are packed in the teflon capsule, 6ϕ in diameter and 20 mm in length. This capsule wound with r.f. coil was inserted into the water-sealed cylindrical copper container. The copper container was set in the cylindrical vacuum bottle which was laid between the pole pieces (300 mm in diameter, 44 mm in pole gap). The temperature was measured by means of a copper-constantan thermocouple junction placed on the outside of the copper container. Splitting widths of NMR spectrum vary with temperature, so that the lack of uniformity of the sample temperature results in broad (NMR) spectrum. It is necessary for obtaining well-split spectrum to control the sample temperature uniformly. The use of copper container, which had large heat capacity and good heat conduction, gave low temperature fluctuation and good temperature uniformity of the whole sample. The temperature of the sample could be controlled precisely within ± 0.1 K by the circulation of the heat transferable water in vacuum bottle.

In this experiment NMR spectra were recorded using the Pound and Knight type oscillating circuit. And the static magnetic field H_0 and sweep rate were set to 4930 G (the resonance frequency was 21 MHz) and 1.26 G/min, respectively. With decreasing the modulation amplitude NMR spectrum becomes split, so that the modulation amplitude is needed to select the most probable one which gives split spectrum with good S/N ratio. In the apparatus of this experiment, modulation amplitude could be varied from 2 to 0.01 G. The NMR spectra which is presented in the following Chapter were obtained at 0.3 G.

2.3 Raman spectroscopy

Raman spectra were recorded over the range $50 \sim 650\ \mathrm{cm}^{-1}$ using the double monochrometer of Japan Spectroscopic Co. and Ar^+ laser ($\lambda = 4880$ Å) as the light source. As shown in Figure 1, sample was enclosed in a cylindrical glass capsule which is 4 mm in inner diameter and about 25 mm in length. The top of this glass capsule is sealed to avoid the moisture in the air. And to decrease the scattering light of incident laser beam on the surface of the glass capsule, the bottom of which is concaved. This capsule was set in the cylindrical brass block which can be controlled at the temperature from -30°C to 90°C by sheathed heater and cooling tube in which cooling fluid can be circulated. A strong laser beam tends to damage the liquid crystal sample, so it is necessary to obtain the needed scattered intensity with low incident beam intensity. In this apparatus the incident laser beam enters the bottom and passes along the central axis of this cylindrical capsule. With this geometry long light path is obtained in the sample

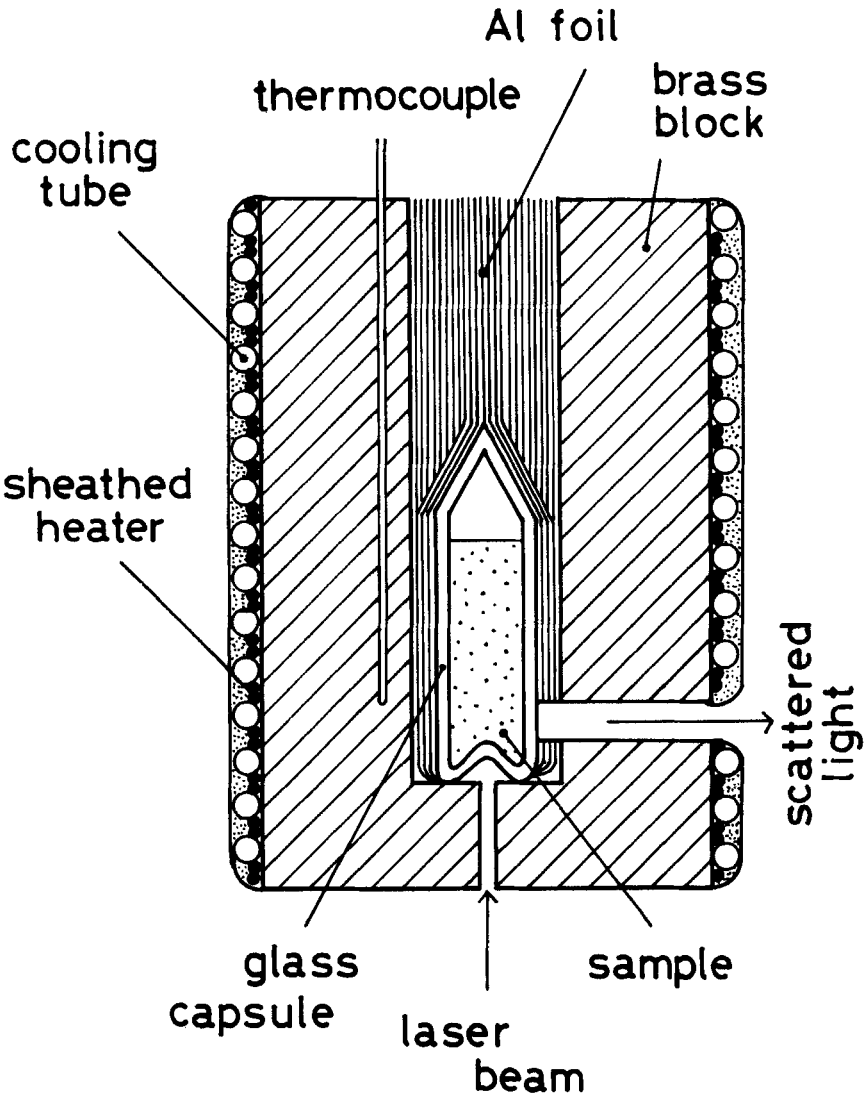

FIGURE 1 Schematic figure of sample cell for Raman Spectroscopy.

and therefore highly scattered intensity was obtained. For collecting more of scattered light and heat transmission, the glass capsule may be covered with aluminium foil and the scattered light is collected through one aperture on the aluminium foil and a hole of the brass block.

3 RESULTS AND DISCUSSION

3.1 Broad line NMR spectra

Broad line NMR spectra (first derivative) of MBBA and EBBA in the nematic phase are shown in Figures 2(a) and (b), respectively. By the adjustment of experimental conditions refined spectra with good S/N ratio could be obtained. As shown in Figure 2 resonance lines are assigned by the symbols A $\sim$ G.

Watkins and Johnson[17] have reported a NMR spectrum of MBBA. Prasad[22] has obtained the NMR spectra of (nondeuterated) EBBA and deuterated EBBA molecules. The spectra of MBBA and EBBA have summarily two components and are not so refined ones, which are shown in Figure 2. And the most part of the reported NMR spectra for various compounds[13–22] is two or three component spectrum. If high modulation amplitude (for example 1.0 G) was used in the apparatus of this experiment, the resonance spectra of Figure 2 change into a broad two-component spectrum. From this fact it is supposed that the main reason of appearance of broad two component resonance spectra comes from the use of high modulation amplitude.

Figures 3(a) and (b) show the temperature dependencies of the splitting widths of MBBA and EBBA, respectively. Notations on the curves described in Figure 3 follow those of Figure 2. The protons attached to the slow molecular motion parts (such as aromatic ring) contribute to the large splitting widths, and to the fast molecular motion parts (such as end groups) contribute to the narrow splitting widths. Accordingly it is roughly assigned that A, B and C lines of MBBA and A and B lines of EBBA in Figure 2 correspond to the many protons of end groups. Especially the sharp resonance line in the center of each NMR spectrum in Figure 2 comes from the end $-CH_3$ protons with fast segmental motion part. By the analyses of segmental motion and conformation of end groups, the assignment of other resonance lines in the central part of the spectrum and the reason why the central peaks of EBBA are not split as those of MBBA, may be obtained. However, the end proton systems are too complex to analyze. Therefore, the temperature dependencies of narrow splitting widths which seem to attribute to the protons of end groups are omitted in Figure 3. Figure 3 shows the

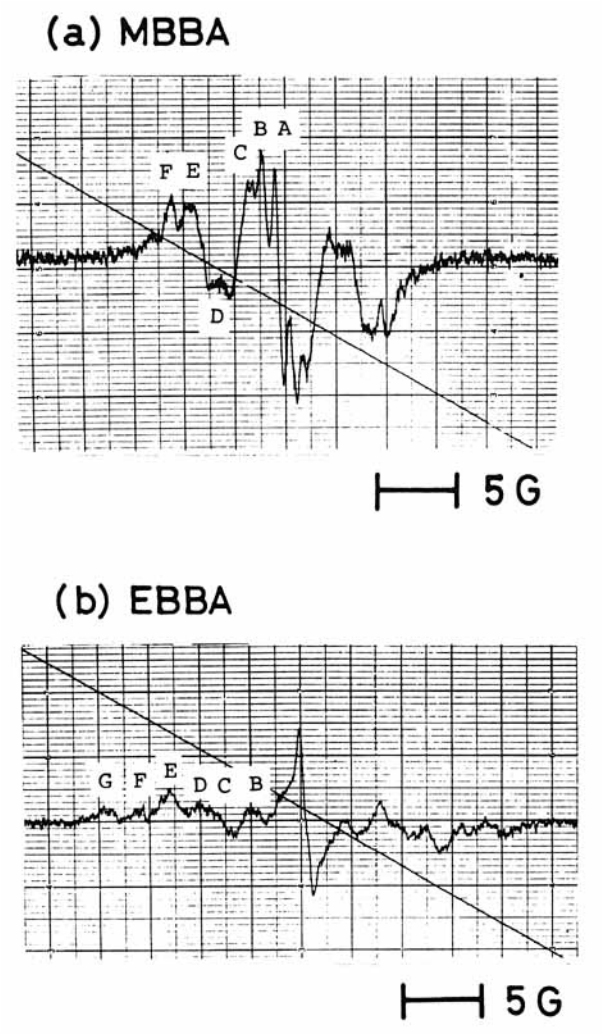

FIGURE 2 Broad line NMR spectra of (a) MBBA and (b) EBBA in the nematic phase. Each resonance line is assigned by symbols A ~ G. The scale bars represent 5 G.

temperature dependencies attributed to the protons of aromatic ring and azomethin (—CHN—) group of both molecules. As shown in Figure 3, with increasing the temperature, each splitting width decreases in the same way. This result shows that segmental motions of aromatic ring and azomethin group become active uniformly with increasing the temperature. These tendencies of segmental motions of MBBA and EBBA are similar to each other.

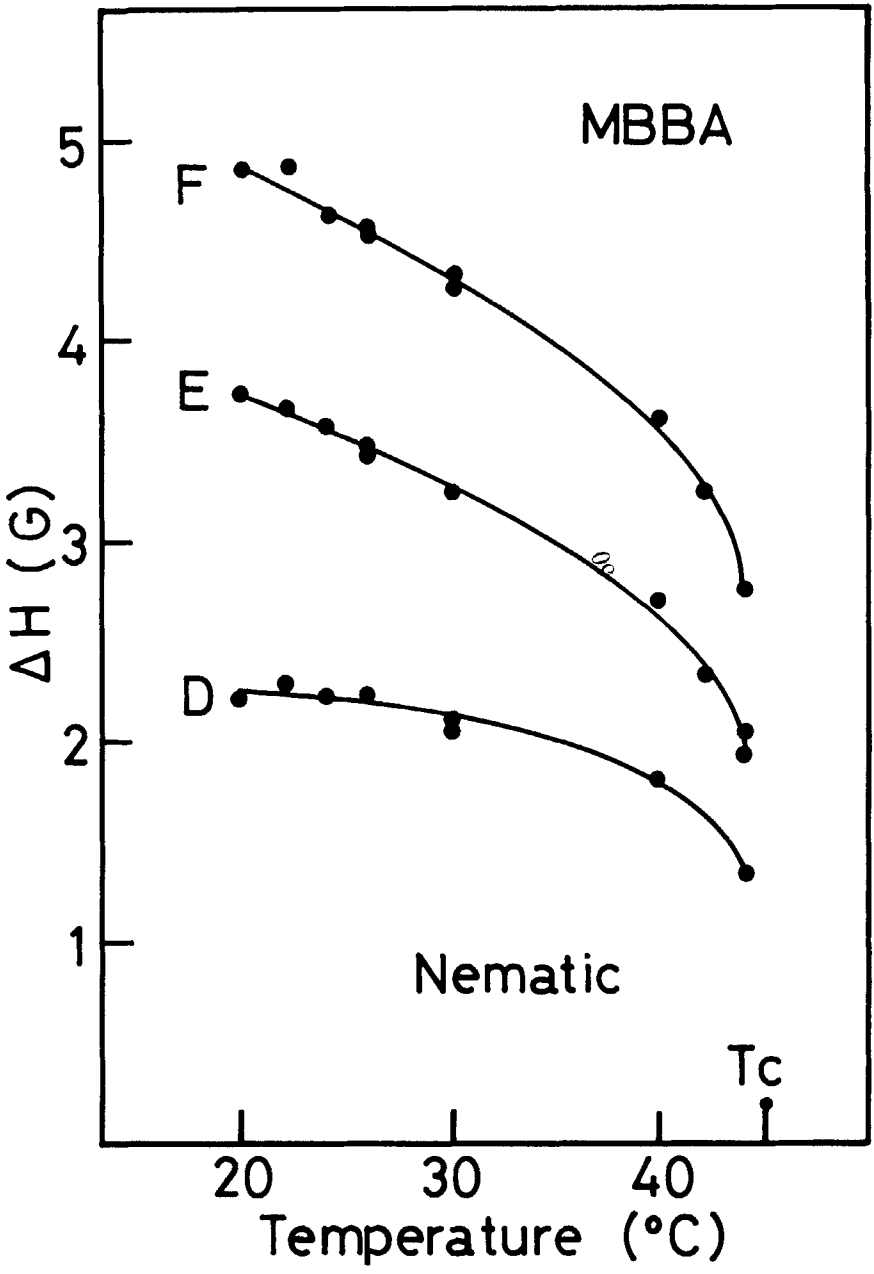

(a)

FIGURE 3 Temperature dependencies of the splitting widths of (a) MBBA and (b) EBBA. Notations on the curves follow those of Figure 2.

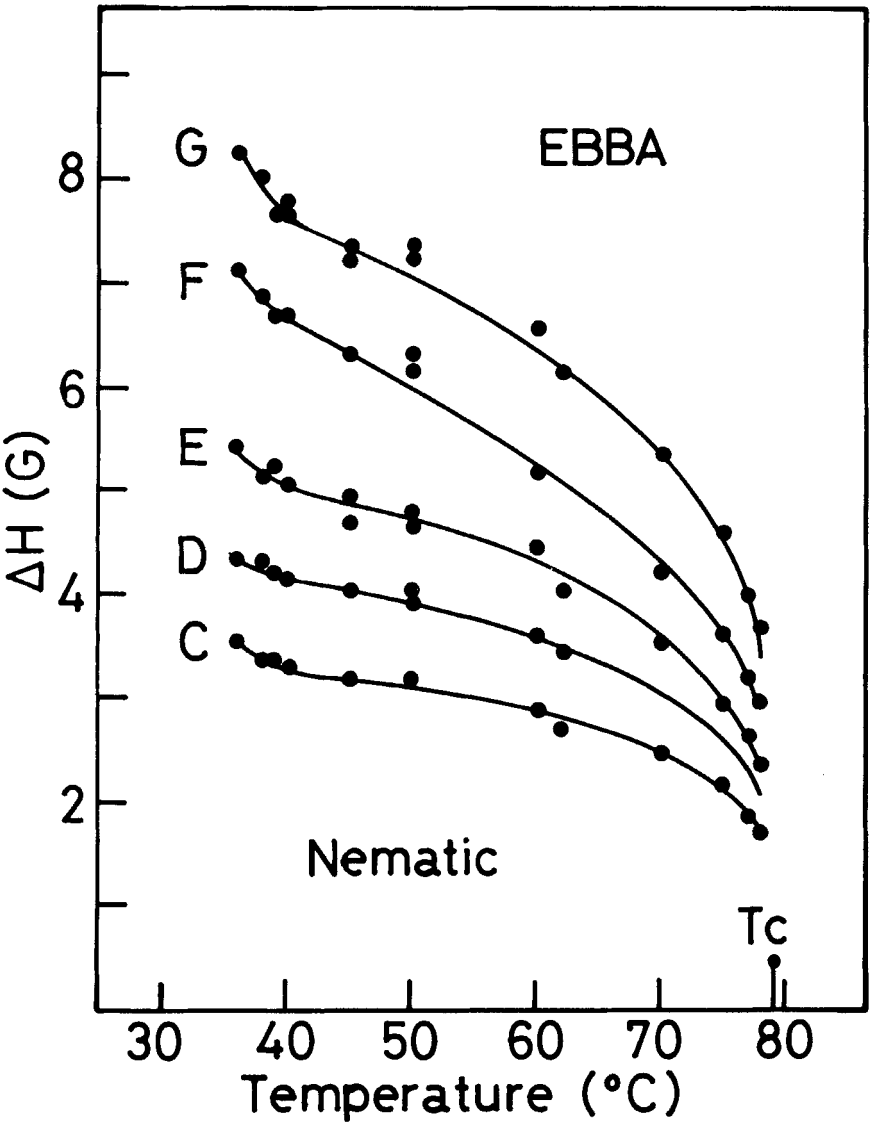

(b)

On the other hand, the splitting widths of EBBA are larger than those of MBBA. Since in the nematic state intermolecular interactions are motionally averaged, protons which belong to other molecules have no contribution to the NMR spectra. Thus large splitting widths of EBBA indicate the large interproton interactions in the intramolecule. The conformation of the benzylideneaniline parts seems to be nearly similar in both MBBA and EBBA molecules, so that large splitting widths of EBBA should be explained by the difference of the conformation of end chains, especially of the butyl chain which has the protons that are located in the nearest position to the protons of aromatic ring. The conformational difference of the end butyl chain cannot be obtained directly from these NMR spectra. Further analysis of splitting widths of NMR spectra is made by the aid of conformational analysis described both in Section 3.2 and in Section 3.3.

3.2 RAMAN SPECTROSCOPY

3.2.1 Raman spectra It has been reported[27] that accordion mode vibration in liquid crystal is observed in the $200 \sim 400\,cm^{-1}$ region as a whole. Behroozi *et al.*[28] studied the accordion bands in the Raman spectra of homologous series of n-alkylbenzenes in the solid and liquid phase. They have suggested that accordion mode of the end butyl chain of n-butylbenzene is assigned to the band at $280\,cm^{-1}$. In n-butylbenzene it is supposed that benzene ring behaves like the nodal point of accordion mode vibration of the end butyl chain because of the large mass of benzene ring. Accordingly it is also supposed that accordion mode vibration is affected to a small extent by the substitution of other radical at the para position of n-butylbenzene. In this investigation, detecting the accordion mode vibration of the end butyl chain of MBBA and EBBA Raman spectroscopy was carried out in the $100 \sim 470\,cm^{-1}$ region.

The Raman spectra of liquid phase of MBBA and EBBA were similar to those of nematic phase. The spectra of solid and nematic phase of MBBA were similar to those of solid and liquid phase shown by Vergoten *et al.*[8] respectively, so the spectra of MBBA are not shown here. Figure 4 shows the Raman spectra of nematic and solid phase of EBBA, which were obtained at 43°C and 17°C respectively. For the assignment of accordion mode vibration, Raman spectra of n-butylbenzene and n-butylaniline were obtained at the room temperature and are shown in Figure 5.

3.2.2 Assignment of accordion mode vibration of end butyl chain As shown in Figure 5, peaks can be observed at about $280\,cm^{-1}$ in n-butylbenzene

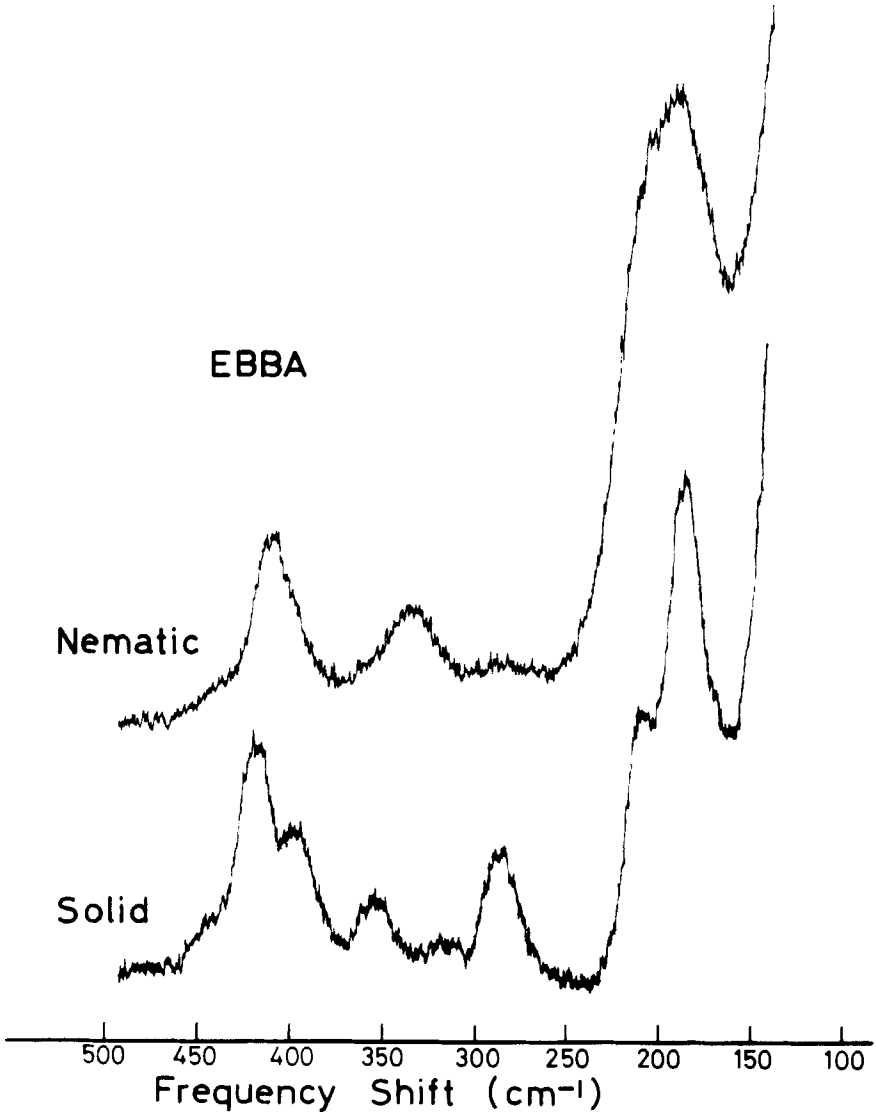

FIGURE 4 Raman spectra of EBBA in the solid (17°C) and nematic (43°C) phase. Raman spectrum in the liquid phase is similar to that of nematic.

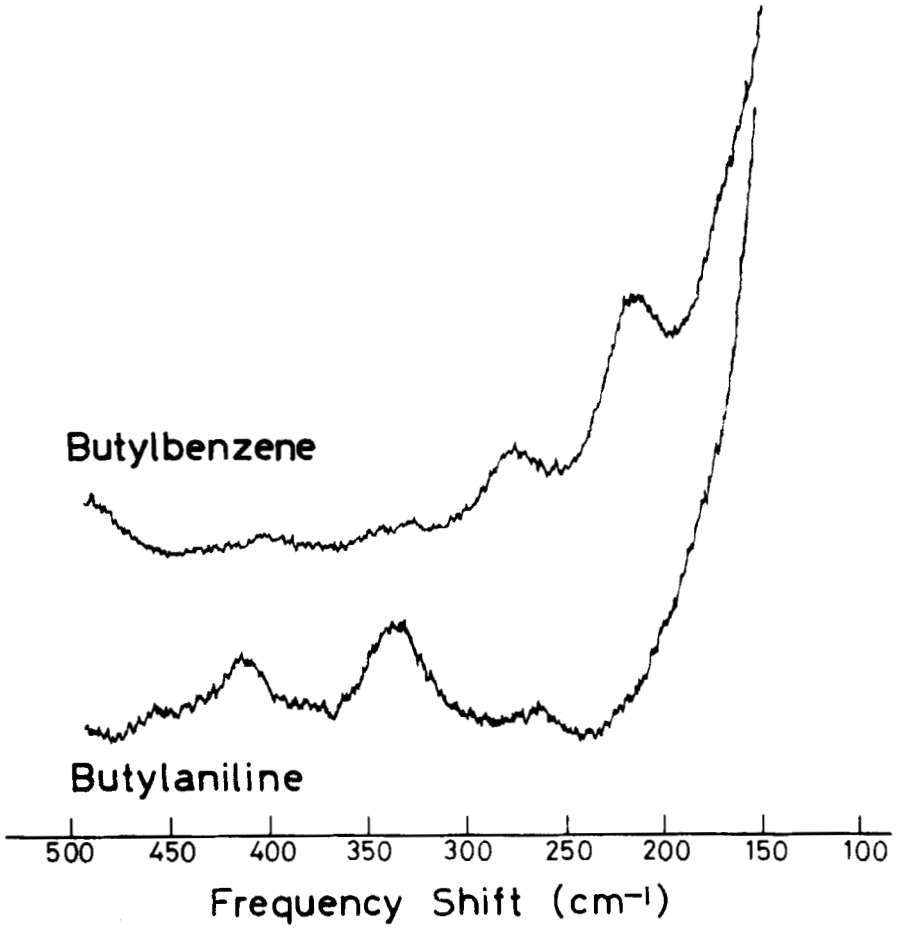

FIGURE 5 Raman spectra of (a) butylbenzene and (b) butylaniline at the room temperature (liquid state).

and also in n-butylaniline. The difference of chemical structure between n-butylbenzene

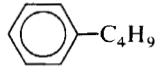

and n-butylaniline

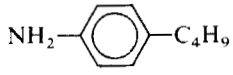

is seen only in $-NH_2$ group. It is easily supposed that $-NH_2$ group does not affect accordion mode vibration, and that the intensity of accordion mode vibration does not change so much in the spectra of these two materials. The peaks of 340 cm^{-1} and 410 cm^{-1} in the spectrum of n-butylaniline disappear in the spectra of liquid and solid[28] of n-butylbenzene, so that the peaks cannot be assigned to the accordion mode vibration. Accordingly it can be concluded that only the 280 cm^{-1} band corresponds to the accordion mode vibration of the end butyl chain. This assignment coincides with what is suggested by Behroozi *et al.*[28] who observed Raman spectra of solid and liquid n-alkylbenzene homologous series.

In the nematic and isotropic phases of MBBA and EBBA, by the increase of molecular motion a certain part of the end butyl chain takes gauche conformation. Since accordion band exists only in the all trans conformation of the end butyl chain, the band, which decreases in intensity on melting, can be identified as an accordion band. In the Raman spectra of stable solid form of EBBA (Figure 4), the intensity of the peak at about 280 cm^{-1} decreases considerably in the nematic and isotropic phases. Consequently accordion band of the end butyl chain of EBBA can be assigned to the peak which exists at about 280 cm^{-1}. This assignment coincides with that obtained in n-butylbenzene and n-butylaniline, and therefore it can be concluded that the accordion band of the end butyl chain exists at about 280 cm^{-1}.

If this assignment is correct, the quantity of the end butyl chain which takes all trans conformation can be estimated from the intensity of 280 cm^{-1} band. The residual peak at 280 cm^{-1} in the nematic phase of EBBA show that some butyl chains takes all the trans conformations even in the nematic phase.

On the other hand, 280 cm^{-1} band cannot be observed in the spectra of MBBA obtained in this investigation and also in the spectra presented by Vergoten *et al.*[8] and Destrade.[9] Instead of this 280 cm^{-1} band, 310 cm^{-1} band appears in the nematic and isotropic phases as shown in the spectra presented by Vergoten *et al.*, but its intensity decreases in the solid phase. In the Raman spectra of the three solid modifications reported by Destrade,[9] the peaks which seem to correspond to the 310 cm^{-1} band exist in 293 $\sim$ 315 cm^{-1} region. These results can be explained as follows. If constraint from other molecules exist to the bond between benzene ring and butyl chain of MBBA molecule, accordion mode vibration occurs in the end propyl chain. This is the case of nematic and isotropic phase. Accordion mode frequency of n-propylbenzene is 316 cm^{-1} and that of n-butylbenzene is 280 cm^{-1},[28] so that accordion mode frequency exists in the 280 $\sim$ 316 cm^{-1} region according to the strength of its constraint. If constraint exists to another

bond in the butyl chain, the intensity of accordion mode vibration of the end propyl chain decreases. This is the case of solid phase. These explanations are confirmed furthermore in the following section.

3.2.3 Molecular packing in nematic phase Specific volumes of MBBA and EBBA in nematic phase have been reported by Gulari and Chu (MBBA)[2] and Bahadur and Chandra (EBBA).[3,4] As the temperature dependencies of those specific volumes are similar to each other in spite of the difference of nematic range, the comparison of those specific volumes can be estimated at the same reduced temperature (T/Tc). Specific volumes of MBBA and EBBA at the same reduced temperature ($T/Tc = 0.990$) are 0.971 (gm/cm^3) and 1.004 (gm/cm^3), respectively. The difference of the molar volume, which is calculated from these values, results in 23 cm^3/mol. This value (23 cm^3/mol) is given by the addition of —CH_2— unit to MBBA molecule, however, the molar volume of —CH_2— unit which is calculated from crystalline PE and liquid paraffin is in the 14 ~ 18 cm^3/mole range. The value of 23 cm^3/mole is large enough for the addition of —CH_2— unit. These values (specific and molar volume) indicate that EBBA takes loose packing rather than MBBA.

Clearing point can be considered as a measure of the degree of disordering in molecular packing of nematic phase. In spite of the small change of chemical structure, clearing points of MBBA (46°C) and EBBA (79°C) are largely different. According to the review of the clearing point of N-(4-alkoxybenzylidene)-4-butylaniline homologous series,[1] steric (odd-even) effect of alkoxy chain has an important influence on the clearing point. The clearing point of EBBA which is higher than that of MBBA indicates that EBBA molecules pack in the nematic state with smaller constraint from other molecules rather than MBBA. Leadbetter *et al.*[34] have already presented the X-ray diffraction patterns of oriented and unoriented nematic phases of MBBA and EBBA, and have analyzed X-ray diffraction on the basis of the paracrystal theory. They explained that EBBA has a larger correlation length than MBBA, and that MBBA is much worse-ordered along the texture direction. These analyses (specific volume, clearing point and X-ray) lead to the following conclusion as to the molecular packing of MBBA and EBBA in the nematic phase. MBBA molecule takes closed packing with some constraint from other molecules and EBBA molecules pack in well-ordered form with small constraint. If the end butyl chain of MBBA or EBBA molecule takes all trans conformation, the end butyl chain is sterically the most projecting part out of the rod like these molecules. So it is easily supposed that the constraint from other molecules mainly occurs on this end butyl chain part and disturbs all trans conformation. Accordingly it can be explained that the end butyl chain of EBBA molecule tends to take

all trans conformation, and that that of MBBA molecule tends to take the conformation which has constraint, such as gauch conformation. These explanations coincide with that obtained by Raman spectroscopy, so that the correctness of the assignment of accordion mode vibration mentioned in Section 3.2.2 is confirmed.

3.3 Molecular motion in the nematic phase

3.3.1 Theoretical description Theoretical description of the dipolar splitting in NMR spectrum of nematic materials has already been given elsewhere.[15,21,22] So the derivation of the formula is omitted in the present analysis. Notations used in the present analysis are as follows:

ΔH_{jk} splitting width resulted from the dipole–dipole interaction of the two protons, H_j and H_k.

r_{jk} inter proton distance between H_j and H_k.

μ gyromagnetic ratio.

θ_0 angle between the applied magnetic field and preferred orientation of the molecule.

γ_{jk} angle between the para axis of the benzene ring and the line joining the two interacting protons, H_j and H_k.

ϕ angle between the para axis of the benzene ring and the long axis of the molecule.

ξ angle between the preferred orientation of the molecule and the particular molecular axis.

Splitting width and order parameter (S) are given in the following

$$\Delta H_{jk} = 3\mu r_{jk}^{-3} \langle \tfrac{3}{2}\cos^2 \gamma_{jk} - \tfrac{1}{2}\rangle \langle \tfrac{3}{2}\cos^2 \phi - \tfrac{1}{2}\rangle \langle \tfrac{3}{2}\cos^2 \xi - \tfrac{1}{2}\rangle \times \langle 3\cos^2 \theta_0 - 1\rangle \quad (1)$$

$$S = \tfrac{1}{2}\langle 3\cos^2 \xi - 1\rangle \quad (2)$$

At the field above 2000 G, the preferred orientation of the nematic state is along the direction of the magnetic field, i.e. $\theta_0 = 0$. A value for ϕ of 10° is calculated from the molecular model mentioned in Section 3.3.2. Therefore, Eq. (1) results in

$$\Delta H_{jk} = AS\langle \tfrac{3}{2}\cos^2 \gamma_{jk} - \tfrac{1}{2}\rangle r_{jk}^{-3} \quad (3)$$

where A is constant ($A = 80.78\ \text{G}\cdot\text{Å}^3$).

Observed splitting widths are too large to be explained by the two proton system. For the large splitting widths, explanations of dipole-dipole interactions of multi proton system should be done. However the calculation of energy level caused by the dipole-dipole interactions of multi proton system really difficult. Accordingly as the first approximation for analyzing the splitting widths caused by multi proton system, it is assumed that the splitting width ΔH_j of the j-th proton is given by the summation of all splitting widths ΔH_{jk} which are attributed to all the dipole-dipole interaction pairs between the proton H_j and H_k, i.e.

$$\Delta H_j = \sum \Delta H_{jk}. \tag{4}$$

3.3.2 Assignment of NMR spectrum In order to obtain the assignment of each resonance line of Figure 1 to specific proton, the method of the analysis mentioned in Section 3.3.1 applied to the multi proton system of MBBA and EBBA. For the ease of the assignment all protons attached to MBBA and EBBA molecules are assigned with the number as shown in Figure 6. For the lack of X-ray analysis of crystalline MBBA and EBBA, the conformation (bond lengths and bond angles) of each molecule has not been obtained in detail. So in the present calculation, the well-known values[16, 17, 35, 36] are used as to the bond lengths and bond angles. All bond angles of benzylidene aniline part are chosen to be 120°, all C—H bonds 1.08 Å and benzenic C—C bonds 1.04 Å. For the azomethin group; C—N = 1.44 Å, C—N = 1.27 Å and C—C = 1.46 Å. Several authors[21, 22, 35, 36] have given the dihedral angles (1) between the benzylidene ring and azomethin (C—C=N—C) linkage plane and (2) between the butyl-benzene ring and azomethin linkage plane. However the reported angles are somewhat different among these authors. For obtaining the adequate conformation of the benzylideneaniline part above two dihedral angles were changed in the calculation.

In the nematic phase, segmental motions of the end chains are active. Protons attached to the end parts of the end chains, for example $-CH_3$, move freely, so that the dipole-dipole interactions attributed to those parts result in smaller splitting widths. And an interpolation distance between a proton attached to these end parts and a proton attached to the benzene rings are large enough. So the contribution to the splitting width from these end parts of the end chains can be neglected. On the other hand as mentioned in Section 3.1, large interproton interactions exist in EBBA between the protons attached to the butyl chain and the protons attached to the aniline ring. It is supposed that the large interproton interactions are attributed to the protons attached to the stem part of butyl chain, and that the end butyl chain takes somewhat rigid conformation. Accordingly the

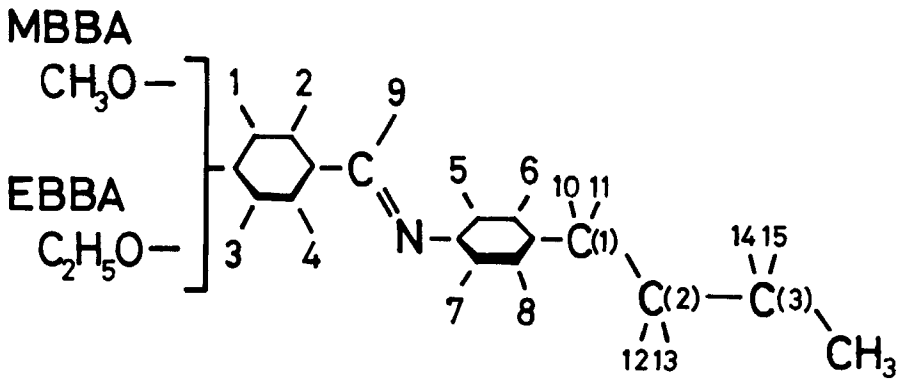

MBBA

	D	E	F
ΔH_j	4·9	7·3	9·5
proton	9	1, 3, 4, 5, 7, 8	2, 6

EBBA

	C	D	E	F	G
ΔH_j	5·6	7·1	8·1	9·9	12·2
proton	9	1, 3	4, 5	2, 7, 6	8

FIGURE 6 Structures of MBBA and EBBA molecule. Each proton is assigned by a number. Table show the assignment of each proton to the resonance line and its calculated splitting width.

contribution to the splitting width from the protons attached to the stem part of end butyl chain should be calculated. However the conformations of end butyl chains of MBBA and EBBA molecule have not been given. To obtain the possible conformation of end butyl chain following three rotational angles were changed. The rotational angles around (3) the aniline—C(1) bond, (4) C(1)—C(2) bond and (5) C(2)—C(3) bond. All

C—C bond lengths of end butyl chain are chosen to be 1.54 Å and all C—H bonds 1.08 Å.

By the use of these bond lengths and bond angles, the calculation of the splitting widths of NMR spectrum was carried out. About five angles were obtained most probably as the calculated splitting widths can explain the splitting widths and number and intensity of the peaks in NMR spectrum. In Figure 6 the assignment of each proton (H_j) to the resonance lines and the calculated splitting widths (ΔH_j) for the protons attached to the benzylideneaniline part are shown. The values of the calculated splitting widths correspond to those of the perfectly ordered state. The calculated splitting widths of each proton are different from each other, but the difference of the splitting widths in the same assignment group in Figure 6 is small. So the value of the splitting width in Figure 6 is the averaged one of the splitting widths in the same assignment group. The probable error of these averaged values are smaller than 4%.

Above dihedral angles (1) and (2) results in 20° and 70°, respectively. From NMR study of deuterated MBBA, Lee *et al.*[21] show that the twist of the aniline ring away from azomethin linkage plane is about 47°. And Prasad[22] shows that the dihedral angle is 43° from NMR study of deuterated EBBA. From X-ray analysis for benzylideneaniline and its derivatives, Bürgi and Dunitz[35,36] have reported that the dihedral angles between the azomethin plane and the aniline and benzylidene rings were 55°–41° and 8°–14°, respectively. The calculated dihedral angle between the benzylidene ring and the aniline ring coincide with reported one. The present calculation shows that the azomethin linkage plane is twist rather than reported one.

The splitting widths were calculated for the various conformations of the end butyl chain, which were caused by the variation of three rotational angles, and all trans conformation was the most probable one. For the explanation of the splitting width of the NMR spectrum of MBBA, the contributions to the splitting widths from the protons 10 and 11 were necessary to calculate with small extent, however, the contribution of other protons attached to the butyl chain was necessary to neglect. On the other hand, for the explanation of the splitting widths of the NMR spectrum of EBBA, the contributions to the splitting widths from the protons 10, 11, 12 and 13 were necessary to calculate fully. These results show that the stem part of the end butyl chain of EBBA molecule attaches to the benzene ring more rigidly with large interproton interactions than that of MBBA, and that the end butyl chain of EBBA molecule tends to take extended all trans conformation rather than MBBA. This conclusion coincides with that obtained by Raman spectroscopy.

From these splitting widths, order parameters $S_D - S_F$ of MBBA and $S_C - S_G$ of EBBA at each temperature can be calculated. Order parameters,

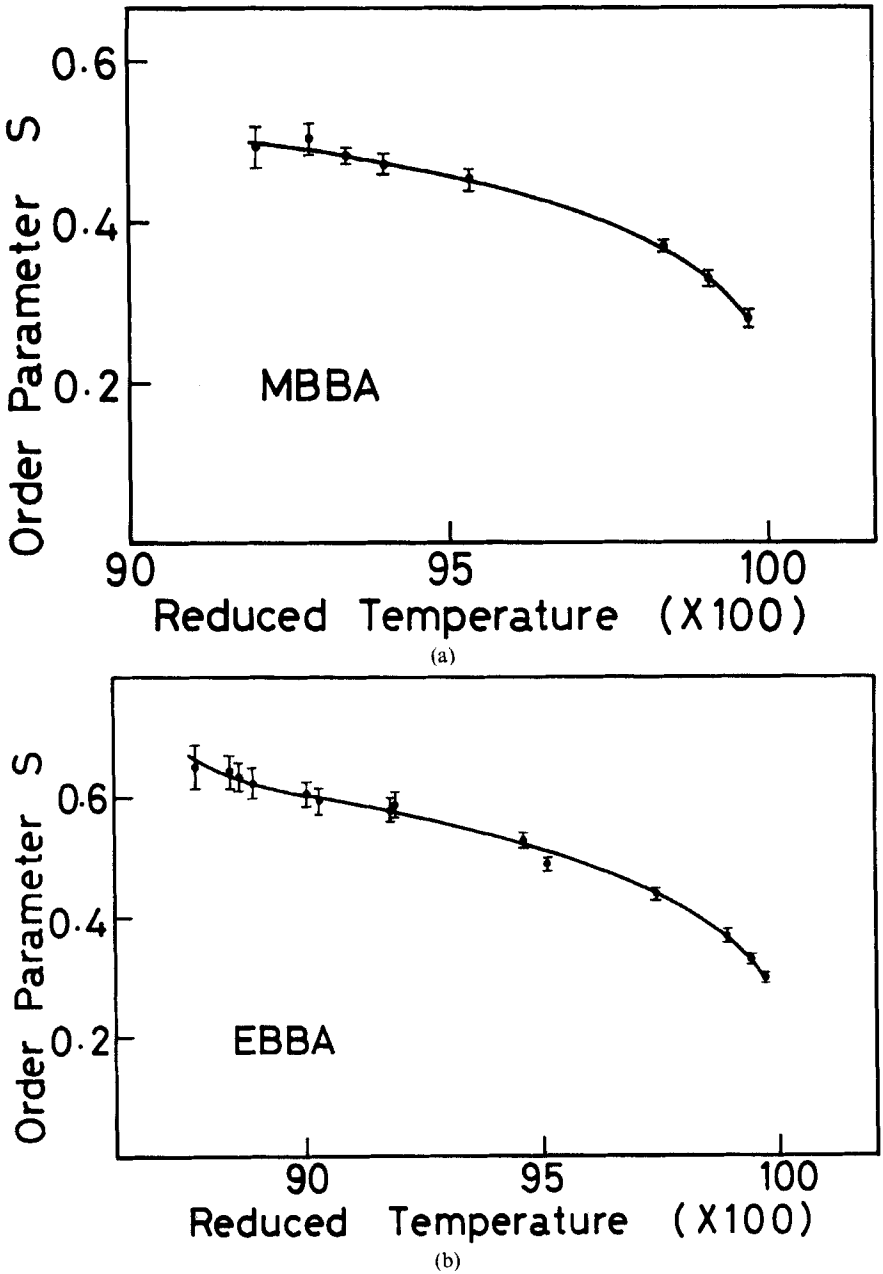

FIGURE 7 Temperature dependencies of the averaged order parameters of (a) MBBA and (b) EBBA. Scale bar described on the curve shows the probable error of the averaged order parameter.

$S_D - S_G$, can be considered as a measure of amplitude of segmental motion. However the calculated order parameter for each splitting width takes nearly the same value at respective temperature, so it is supposed that the amplitude of segmental motions increase uniformly on the whole molecule. So therefore the orientational order parameter of whole molecule, S, can be obtained as an averaged value of each order parameters ($S_D - S_F$) at each temperature. Temperature dependencies of the averaged order parameters of MBBA and EBBA are shown in Figures 7(a) and (b), respectively. Scale bar described on the curve shows the probable error of the averaged order parameter. The probable error is smaller than 5%. The temperature dependency of order parameter has been given theoretically by Maier–Saupe[37] theory. Averaged order parameters obtained in the present experiment approximately coincide with the theoretical one.

Acknowledgements

The authors wish to thank the Grant-in-Aid for Scientific Research from the Ministry of Education for financial support of this work.

References

1. Z. G. Gardlund, R. J. Curtis, and G. W. Smith, *Liquid Crystals and Ordered Fluids* (Plenum, New York, 1974), p. 541.
2. E. Gulari and B. Chu, *J. Chem. Phys.*, **62**, 795 (1975).
3. B. Bahadur and S. Chandra, *J. Phys. Chem. Solid State Phys.*, **9**, 5 (1976).
4. B. Bahadur, *J. Phys.*, **73**, 255 (1976).
5. R. Freyman and R. Servant, *Ann. Phys.*, **20**, 131 (1945).
6. J. M. Schnur, *Phys. Rev. Lett.*, **29**, 1141 (1972).
7. J. M. Schnur, *Mol. Cryst. Liq. Cryst.*, **23**, 155 (1973).
8. G. Vergoten and G. Fleury, *Mol. Cryst. Liq. Cryst.*, **30**, 213 (1975).
9. C. Destrade and H. Gasparoux, *J. Phys. Lett.*, **36**, L-105 (1975).
10. C. Destrade, F. Guillon, and H. Gasparoux, *Mol. Cryst. Liq. Cryst.*, **36**, 115 (1976).
11. F. Cavatorta, M. P. Fontana, and N. Kirov, *Mol. Cryst. Liq. Cryst.*, **34**, 241 (1977).
12. J. Le Brumant, N. A. Tuan, and M. Jaffrain; XII European Congress of Spectroscopy Strasbourg, 1975.
13. R. D. Spence, H. A. Moses, and P. L. Jain, *J. Chem. Phys.*, **21**, 380 (1953).
14. P. L. Jain, J. C. Lee, and R. D. Spence, *J. Chem. Phys.*, **23**, 878 (1975).
15. J. C. Rowell, W. D. Phillips, L. R. Melby, and M. Panar, *J. Chem. Phys.*, **43**, 3442 (1965).
16. N. Bravo, J. W. Doane, S. L. Arora, and J. L. Fergason, *J. Chem. Phys.*, **50**, 1398 (1969).
17. C. L. Watkins and C. S. Johnson, Jr., *J. Phys. Chem.*, **75**, 2451 (1971).
18. J. W. Doane, R. S. Parker, B. Civilk, D. L. Johnson, and D. L. Fishel, *Phys. Rev. Lett.*, **26**, 1694 (1972).
19. M. N. Avadhanlu, J. S. M. Sarma, and C. R. R. Murty, *Ber. Bunsenges. Physik. Chem.*, **77**, 275 (1973).
20. M. N. Avadhanlu and C. R. K. Murty, *Mol. Cryst. Liq. Cryst.*, **20**, 221 (1973).
21. Y. S. Lee, Y. Y. Hsu, and D. Dolphin, *Liquid Crystals and Ordered Fluids* (Plenum, New York, 1974), p. 357.
22. J. S. Prasad, *J. Chem. Phys.*, **65**, 941 (1976).
23. A. Loesche; Proceeding of the International School of Physics "Enrico Fermi" (North-Holland Publishing, New York, 1976), Course LIX, p. 771.

24. A. Saupe and G. Englert, *Phys. Rev. Lett.*, **11**, 462 (1963).
25. R. F. Schaufele and T. Shimanouchi, *J. Chem. Phys.*, **47**, 3605 (1967).
26. R. F. Schaufele, *J. Chem. Phys.*, **49**, 4168 (1968).
27. B. J. Bulkin, *Advances in Liquid Crystals*, Vol. 2, Ed., G. H. Brown (Academic Press, New York, 1976), p. 199 ff.
28. F. Behroozi, R. G. Priest, and J. M. Schnur, *J. Raman Spec.*, **4**, 379 (1976).
29. J. Meyer, T. Waluga, and J. A. Janik, *Phys. Lett.*, **41A**, 102 (1972).
30. J. E. Lydon and J. O. Kessler, *J. Phys. Lett.*, **36**, CL-153 (1975).
31. M. Sorai, T. Nakamura, and S. Seki, *Bull. Chem. Soc. Japan*, **47**, 2192 (1974).
32. K. Z. Ogorodnik, *Mol. Cryst. Liq. Cryst.*, **42**, 53 (1977).
33. M. Yasuniwa and K. Minato, *The Research Reports of Kurume Technical College*, **32**, 39 (1979).
34. A. J. Leadbetter, R. M. Richardson, and C. N. Colling, *J. Physique*, **36**, CL–37 (1975).
35. H. B. Bürgi, J. D. Dunitz, and C. Zust, *Acta Crystallogr.*, **B24**, 463 (1968).
36. H. B. Bürgi and J. D. Dunitz, *Chem. Commun.*, **472** (1969).
37. W. Maier and A. Saupe, *Z. Naturforsch.*, **14a**, 882 (1979); ibid **15a**, 287 (1960), **16a**, 816 (1961).